A Novel Flex-Stretch-Flow Bioreactor for the Study of Engineered Heart Valve Tissue Mechanobiology

George C. Engelmayr Jr.,[1] Lorenzo Soletti,[1] Sarah C. Vigmostad,[2] Stephanus G. Budilarto,[1] William J. Federspiel,[1] Krishnan B. Chandran,[2] David A. Vorp,[1] and Michael S. Sacks[1]

[1]Department of Bioengineering, McGowan Institute for Regenerative Medicine, University of Pittsburgh, 100 Technology Drive, Suite 200, Pittsburgh, PA 15219, USA; and [2]Department of Biomedical Engineering, College of Engineering, The University of Iowa, Iowa City, IA 52242, USA

Abstract—Tissue engineered heart valves (TEHV) have been observed to respond to mechanical conditioning *in vitro* by expression of activated myofibroblast phenotypes followed by improvements in tissue maturation. In separate studies, cyclic flexure, stretch, and flow (FSF) have been demonstrated to exhibit both independent and coupled stimulatory effects. Synthesis of these observations into a rational framework for TEHV mechanical conditioning has been limited, however, due to the functional complexity of trileaflet valves and the inherent differences of separate bioreactor systems. Toward quantifying the effects of individual mechanical stimuli similar to those that occur during normal valve function, a novel bioreactor was developed in which FSF mechanical stimuli can be applied to engineered heart valve tissues independently or in combination. The FSF bioreactor consists of two identically equipped chambers, each having the capacity to hold up to 12 rectangular tissue specimens ($25 \times 7.5 \times 1$ mm) via a novel "spiral-bound" technique. Specimens can be subjected to changes-in-curvature up to 50 mm^{-1} and uniaxial tensile strains up to 75%. Steady laminar flow can be applied by a magnetically coupled paddlewheel system. Computational fluid dynamic (CFD) simulations were conducted and experimentally validated by particle image velocimetry (PIV). Tissue specimen wall shear stress profiles were predicted as a function of paddlewheel speed, culture medium viscosity, and the quasi-static state of specimen deformation (i.e., either undeformed or completely flexed). Velocity profiles predicted by 2D CFD simulations of the paddlewheel mechanism compared well with PIV measurements, and were used to determine boundary conditions in localized 3D simulations. For undeformed specimens, predicted inter-specimen variations in wall shear stress were on average ±7%, with an average wall shear stress of 1.145 dyne/cm^2 predicted at a paddlewheel speed of 2000 rpm and standard culture conditions. In contrast, while the average wall shear stress predicted for specimens in the quasi-static flexed state was ~59% higher (1.821 dyne/cm^2), flexed specimens exhibited a broad intra-specimen wall shear stress distribution between the convex and concave sides that correlated with specimen curvature, with peak wall shear stresses of ~10 dyne/cm^2. This result suggests that by utilizing simple flexed geometric configurations, the present system can also be used to study the effects of spatially varying shear stresses. We conclude that the present design provides a robust tool for the study of mechanical stimuli on *in vitro* engineered heart valve tissue formation.

Keywords—Tissue engineering, Bioreactor, Heart valve, Flexure, Tension, Flow, Fluid shear stress.

INTRODUCTION

Surgical interventions to repair damaged cardiovascular structures (e.g., vessels, valves, myocardium) are currently limited by the inferior biocompatibility of non-viable prosthetics, and by the scarcity, morbidity (autologous), and potential immunogenicity (allogenic, xenogenic) of donor tissues. Moreover, in pediatric applications current approaches cannot account for somatic growth, leading to multiple re-operations until adulthood with associated morbidity and mortality risks. Tissue engineering (TE) seeks to circumvent these limitations via the *in vitro* construction of autologous tissues using cells and bioresorbable scaffolds.[18] For example, by seeding bone marrow-derived mesenchymal stem cells (BMSC) onto nonwoven scaffolds, Sutherland *et al.*[23] recently constructed tissue engineered heart valves (TEHV) that functioned in the pulmonary outflow tract of sheep for at least 8 months. Optimizing the mechanical properties of TEHV for long-term durability, however, demands a quantitative understanding of the engineered tissue formation process.[22] In particular, the role of mechanical stimulation has yet to be adequately characterized for rational application in TEHV designs.

Address correspondence to Michael S. Sacks, Department of Bioengineering, McGowan Institute for Regenerative Medicine, University of Pittsburgh, 100 Technology Drive, Suite 200, Pittsburgh, PA 15219, USA. Electronic mail: msacks@pitt.edu

George C. Engelmayr, Jr. and Lorenzo Soletti are contributed equally.

While rudimentary aspects of TEHV development (e.g., cell proliferation, collagen secretion) can be stimulated *in vitro* by growth factors,[9] higher level tissue morphogenesis (e.g., formation of dense collagenous layers[21]) has yet to be observed without mechanical stimulation. The pleiotropic actions of mechanical stimulation can both accelerate the *de novo* synthesis of collagen,[6,13,16] as well as guide its structural organization.[3,4] For example, while DNA and collagen concentrations can approach native-like values over 4 weeks static culture with basic fibroblast growth factor (bFGF),[9] it is only with 3–4 weeks mechanical stimulation that layer stratification begins,[6,11] and not until several months *in vivo* that a tri-layered morphology reminiscent of a native semilunar valve develops.[21,23] While it remains unclear if this tri-layered morphology manifests from host-mediated remodeling or hemodynamics, our collective understanding of vascular adaptation suggests a role for the coupled mechanical stimuli of pulsatile flow.

Pulsatile flow loop bioreactors can provide pressure and flow stimuli to TEHV within the context of their ultimate physiomechanical function.[12] More advanced designs incorporate control algorithms and regulators for independently modulating pressure and flow, thereby allowing for the simulation of sub to supra-physiologic hemodynamic conditions.[10] Thus, for the purpose of mechanically conditioning anatomically shaped TEHV prior to implantation, pulsatile flow[10,12] or pulse duplicator[17] bioreactors are virtually indispensable. However, to systematically quantify how individual modes of mechanical stimulation contribute to the tissue formation and maturation process for specific cell/scaffold combinations, a different bioreactor approach involving multiple specimens and decoupled stimuli is necessary. Toward this goal, we and others have designed bioreactors for investigating the independent effects of cyclic flexure,[5,6] tension,[16] and flow (i.e., fluid shear stress)[13] on TEHV tissue formation *in vitro*.

We previously demonstrated that 3 weeks cyclic flexure of vascular smooth muscle cell (SMC)-seeded nonwoven scaffolds at a frequency of 1 Hz and change-in-curvature ($\Delta\kappa$) of 0.554 mm^{-1} can independently stimulate many aspects of TEHV development observed in pulse duplicators, including increased collagen synthesis with concomitant increases in effective stiffness.[6,7] Interestingly, the increase in collagen content observed in the cyclic flexure vs. static group ($+63\%$)[6] was comparable to that observed by others under 2 weeks application of an estimated 0.1 dyne/cm^2 shear stress by continuous laminar flow ($+50\%$)[13] and significantly less that that observed in pulsatile flow loop bioreactor studies ($+409\%$), in which we estimate the shear stress and $\Delta\kappa$ to be 1 dyne/cm^2 and 0.3 mm^{-1}, respectively.[11] Collectively, these findings suggest that

the individual modes of mechanical stimulation may act synergistically to accelerate or amplify collagen synthesis. Accelerated collagen synthesis is critically important when using scaffolds based on rapidly degrading synthetic polymers such as poly(glycolic acid) (PGA), as the kinetics of scaffold degradation mandate a commensurate rate of tissue formation for the maintenance of structural integrity. To elucidate potential coupling effects, however, it must be possible to controllably decouple and then recombine mechanical stimuli in a single bioreactor.

In the current study a novel bioreactor was developed for the purpose of systematically quantifying the independent and coupled effects of cyclic flexure, stretch, and flow (FSF) on engineered heart valve tissue formation *in vitro*. Cyclic flexure and stretch can be applied to tissue specimens via a linear actuator and novel "spiral-bound" tissue-gripping technique. The FSF bioreactor also generates flow via a magnetically coupled paddlewheel rather than an external pump circuit, providing a closed system to help ensure sterility while maintaining a compact footprint for placement inside a standard cell culture incubator. Computational fluid dynamics (CFD) simulations were conducted to predict the specimen wall shear stress profiles as a function paddlewheel angular velocity, culture medium dynamic viscosity, and the state of specimen deformation (e.g., undeformed or flexed) within the flow field. The CFD model was experimentally validated by particle image velocimetry (PIV).

METHODS

FSF Bioreactor Design

The design methodology and materials of construction used in the FSF bioreactor (Figs. 1 and 2)
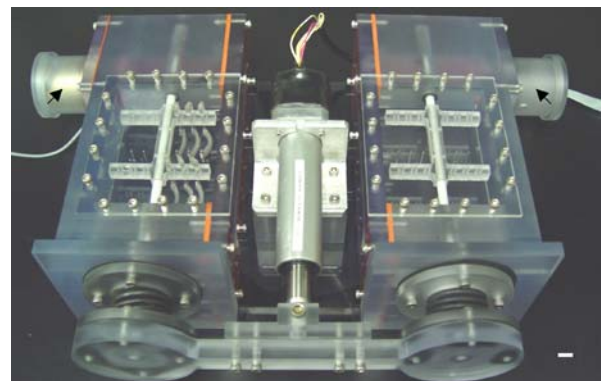

FIGURE 1. FSF bioreactor overview. Photograph (top-front view) of the FSF bioreactor. Cyclic flexure and stretch can be applied to tissue specimens via the centrally positioned linear actuator. The custom-housed magnetic stirrers are located toward the rear of each chamber (black arrows). Scale bar = 1 cm.
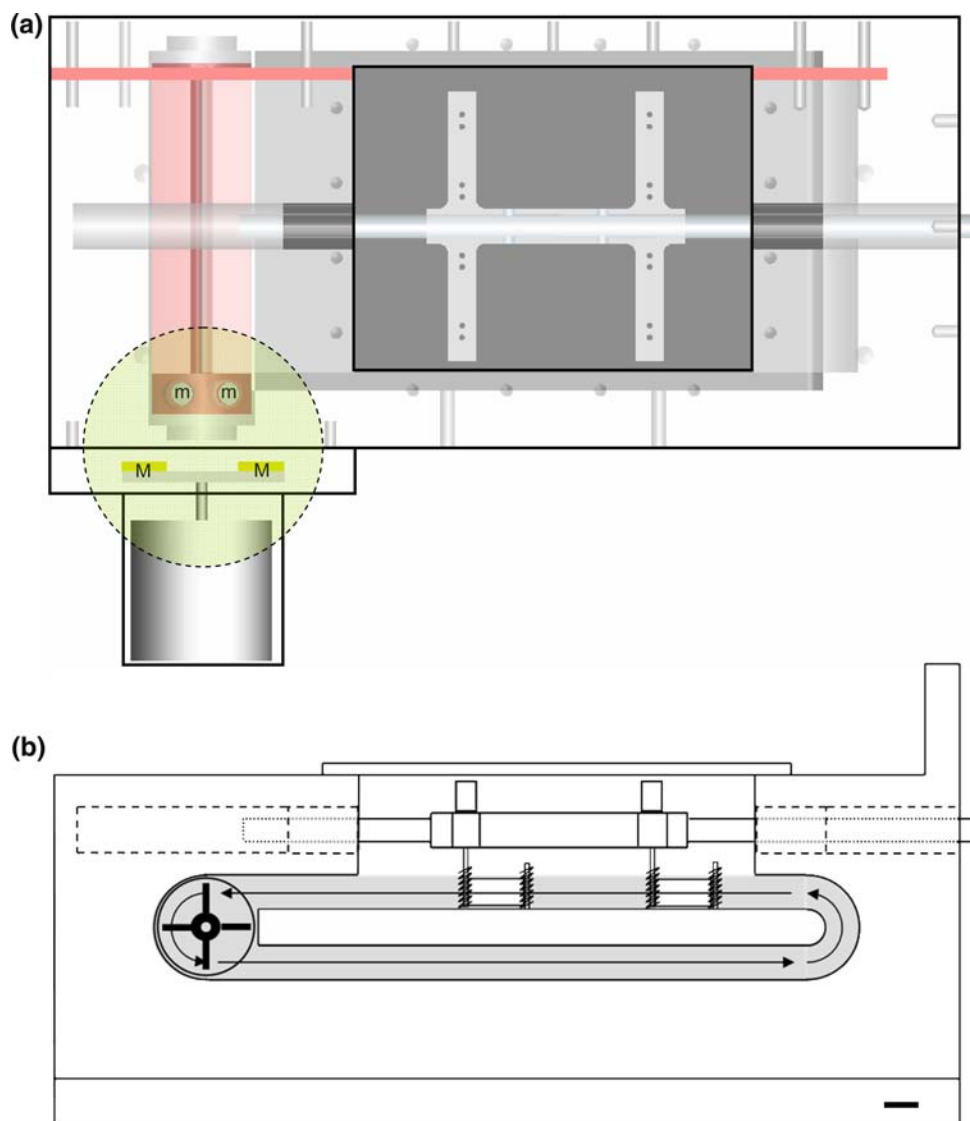
FIGURE 2. FSF bioreactor internal mechanisms. (a) Schematic (top view) of an FSF bioreactor chamber. Neodymium magnets embedded within one end of the paddlewheel (lower case ''m'') couple with neodymium magnets attached to the stirrer motor (uppercase ''M''), thus providing magnetic torque transmission from the stirrer motor to the paddlewheel (dashed circle). (b) Schematic (side view) of an FSF bioreactor chamber. The magnetic stirrer (not shown) attaches to the side of the FSF bioreactor chamber and magnetically couples with the magnets embedded within the paddlewheel. The fluid flow circuit is shaded gray and the direction of culture medium flow is indicated by black arrows. Scale bars = 1 cm.

was based on our previous cyclic flexure bioreactor.[5,6] The structural components of the FSF bioreactor were designed using Solidworks 3D CAD software (Solidworks, Corp., Concord, MA). Machined parts were fabricated from polycarbonate or 316 stainless steel by Astro Automation, Inc. (Irwin, PA). Culture medium can be recirculated within the FSF bioreactor (black arrows) by a magnetically coupled paddlewheel (Fig. 2). The paddlewheel was fabricated by high resolution stereolithography (FineLine Prototyping, Inc., Raleigh, NC) using a Viper Si2™ SLA® system (3D Systems Corp., Valencia, CA) and a high strength, water resistant resin (ProtoTherm 12120™; DSM

Somos®, Newcastle, DE). Two cylindrical (1/4 × 3/4 in.) nickel-coated, grade N38 neodymium (NdFeB) magnets (K&J Magnetics, Inc., Jamison, PA) were press-fit into prefabricated slots on one side of the paddlewheel. The magnets were oriented with their poles in the same direction. Synthetic sapphire ring jewel bearings (Bird Precision, Waltham, MA) were press-fit into either side of the paddlewheel to provide the low starting torque and friction characteristics necessary for effective magnetic torque transmission. The ring jewel bearings couple with stainless steel pivots protruding from the walls of the FSF bioreactor. The paddlewheels are magnetically driven by

immersible magnetic stirrers (Model 75 mm; Corning) fitted into customized polycarbonate housings (Fig. 1; black arrows, Fig. 2a) designed to attach to the side of each FSF bioreactor chamber. The stock magnets of the stirrers were replaced by two rectangular ($1/2 \times 1/2 \times 1/8$ in.) gold-coated, grade N38 neodymium (NdFeB) magnets (K&J Magnetics, Inc.) to improve torque transmission. The stirrer motor has an angular velocity range of 350–2000 rpm controllable by a potentiometer-based speed controller.

The bioreactor consists of two identical chambers, each having an operating fluid capacity of ~300 mL and containing 12 stainless steel "stationary posts" to which tissue specimens can be affixed (Fig. 3). To attach specimens we developed an inexpensive yet highly effective "spiral-bound" tissue-gripping technique. Spiral grips were fabricated by manually winding a length of stainless steel wire (316 V, 0.009″ diameter; Small Parts, Inc., Miami Lakes, FL) about a 2 mm diameter steel mandrel using a drill. Grips were cut to length (~8 mm) and threaded onto both sides of specimens (Fig. 3a; black arrows). The device can thus accommodate a total of 24 rectangular samples (~$25 \times 7.5 \times 1$ mm). Cyclic flexure and/or stretch can be applied by an environmentally sealed linear actuator (UltraMotion, Mattitick, NY), which is rigidly coupled to a cross-arm in the form of a T-junction. Conversely, the cross-arm is rigidly coupled to two shafts, one of which penetrating into each of the two chambers where they actuate a set of "movable posts" (Fig. 3). To reduce the possibility of contamination at these sites of chamber ingress, neoprene rubber bellows (Minor Rubber Co., Bloomfield, NJ) were installed over the shafts to form a seal between the cross-arm and the walls of each chamber. Frequency, amplitude, acceleration, and deceleration profiles can be programmed using Windows-based Si Programmer software (Applied Motion Products, Watsonville, CA). The structural elements of the device can be cold gas sterilized by ethylene oxide, and the entire device was designed to be operated inside of a standard humidified incubator.

Change-in-Curvature Measurement

In the FSF bioreactor, specimens are essentially buckled in order to apply flexural deformations. This is in contrast to our previous cyclic flexure bioreactor, in which specimen flexural deformations were controlled by 3-point bending.[5,6] To quantify the inter-specimen variability in $\Delta\kappa$ in the FSF bioreactor, a full load of 12 scaffold specimens was subjected to a particular deformation and imaged (e.g., Fig. 3c). We have previously utilized a $\Delta\kappa$ of ~0.554 mm^{-1} in our 3-point
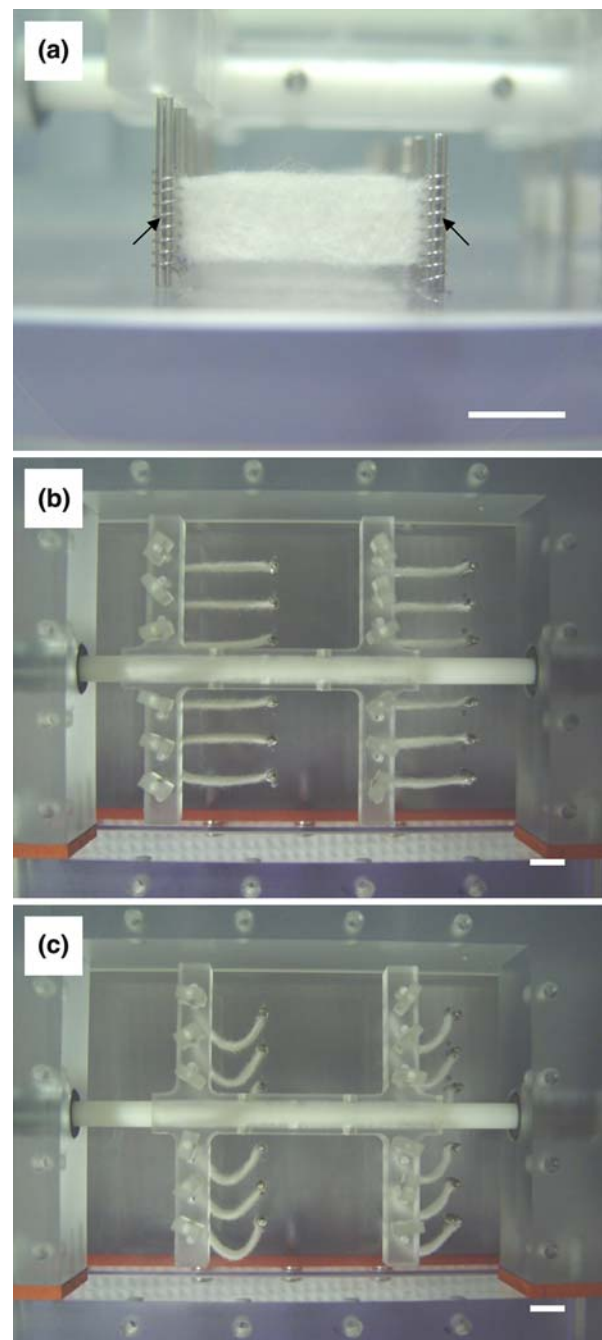

FIGURE 3. Spiral-bound gripping method. (a) Photograph of a nonwoven scaffold specimen "spiral-bound" between stationary and movable posts (black arrows). Stainless steel wire (316 V, 0.009″ diameter; Small Parts, Inc., Miami Lakes, FL) was manually turned using a drill and mandrel (2 mm diameter) to form the spiral tissue binders. The binders were then threaded through the scaffold specimens. (b) Photograph of scaffold specimens in the undeformed configuration. Scaffold specimens can be subjected to cyclic tensile loading by moving the movable posts to the left via the linear actuator (not shown). (c) Photograph of scaffold specimens subjected to a flexural deformation. Scaffold specimens can be subjected to cyclic flexural loading by moving the movable posts to the right via the linear actuator (not shown). Scale bars = 1 cm.

bending cyclic flexure bioreactor,[5,6] as well as in a concurrent study utilizing the FSF bioreactor.[8] The linear actuator was programmed to apply a $\Delta\kappa$ of 0.554 mm^{-1} and an intermediate value of 0.277 mm^{-1}. The resultant $\Delta\kappa$ of each of the visible specimens (10/12) was then computed by first calibrating the image to a scale bar (i.e., converting pixels to millimeters), tracing the shape of the specimens using the trace measurement function of SigmaScan Pro (SPSS Inc., Chicago, IL), and then fitting the traced points using a quadratic equation. $\Delta\kappa$ of the resultant quadratic equations were then computed using Mathcad (Mathsoft) and the equation:

$$\Delta\kappa = \frac{y''}{(1 + y'^2)^{3/2}} - \kappa_0 \qquad (1)$$

where κ_0 is the scaffold specimen's initial curvature, which is 0 since the specimen is initially flat.

Particle Image Velocimetry

The particle image velocity (PIV) device used to experimentally quantify the flow field generated by the paddlewheel has been described previously.[2] In brief, the FSF bioreactor was filled with a solution of neutrally buoyant fluorescent polymer micro-spheres (35-6C, Duke Scientific, Palo Alto, CA) in 37 °C water. The paddlewheel angular velocity was set to a predetermined value (350, 500, 1000, 1500, 2000 rpm) using a non-contact digital laser tachometer (ST6236B; Reed Instruments, Quebec, Canada). The FSF was then positioned for visualization by the PIV device (Fig. 4). A Nd:YAG laser system (Solo PIV III 15 Hz, New wave Research Inc., Fremont, CA) emitting a 532 nm laser pulse was focused into a 2 mm thick sheet using a cylindrical lens (Edmund Optics, Barrington, NJ), and was projected into the FSF from above (note that a temporary transparent lid was positioned directly atop the fluid to mimic the configuration of the 2D CFD simulations). Particles were imaged through the transparent side of the FSF by a Kodak CCD camera (Megaplus ES 1.0, Eastman Kodak Company, San Diego, CA), a close-up lens (60 mm f2.8D AF Micro-Nikkor, Nikon, Japan), and XCAP-standard v.2.2 imaging software (EPIX Inc, Buffalo Grove, IL). Sets of two sequential images were captured within microseconds using the triggered double exposure mode of the camera, a frame grabber (PIXCI® D2X, EPIX Inc, Buffalo Grove, IL), and an eight analog output data acquisition card (NI-6713, National Instruments, Austin, TX). Images thus acquired were analyzed using custom software to extract the velocity profiles for subsequent comparison with CFD simulations.
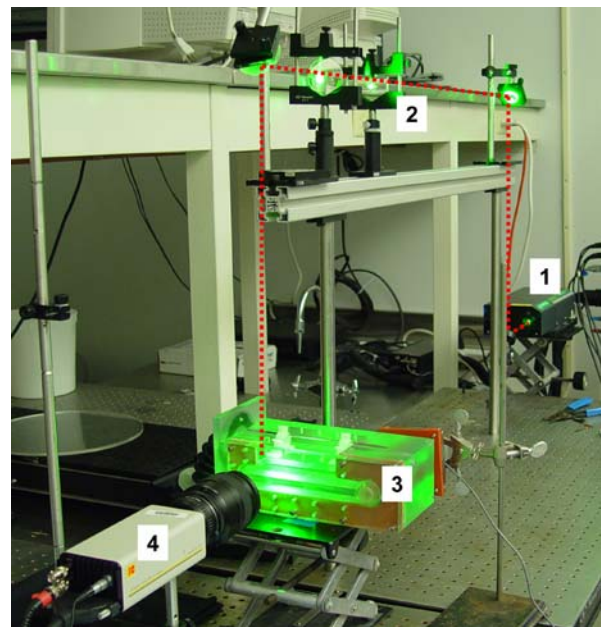

FIGURE 4. Particle image velocimetry (PIV) setup for experimental validation of the 2D CFD model. The PIV device and experimental methods have been described previously in Budilarto *et al.*[2] The pulsed laser (1) was directed by a series of mirrors and lenses (2) into a laser sheet and directed into the top of the FSF bioreactor (3). The camera (4) imaged the laser-illuminated particles. The path of the laser sheet is highlighted by a red dashed line.

CFD Simulations

To quantify the flow rate and fluid shear stress patterns generated by the novel paddlewheel flow system, we developed a computational fluid dynamics (CFD) model using GAMBIT® (v2.1) and FLUENT® (v6.2) software (Fluent, Inc., Lebanon, NH). The geometry of the paddlewheel and associated components of the FSF Bioreactor bath were exported from Solidworks® (Solidworks, Corp., Concord, MA) as ACIS files, reconstructed, adapted, and meshed in the preprocessor GAMBIT. For simulating the relationship between paddlewheel rotational velocity and flow rate, a two-dimensional (2D) model was developed in GAMBIT using a dynamic mesh of ~50,000 triangular elements with size functions applied in proximity of the paddlewheel (Fig. 5a) to represent the motion of the rotating paddlewheel within its casing. The longitudinal median section of the 3D model was used for this purpose due to its symmetry. The geometry was completely closed (all "wall" surfaces, or no slip condition) and the spinning paddlewheel was the sole source of flow generation. Unsteady-state simulations were solved using FLUENT and time steps consistent with a Courant-Friedrichs-Levy (CFL) condition of 0.1 (the time steps depended on the rpm; on average, the time step was ~0.1 ms). The time zero in each simulation
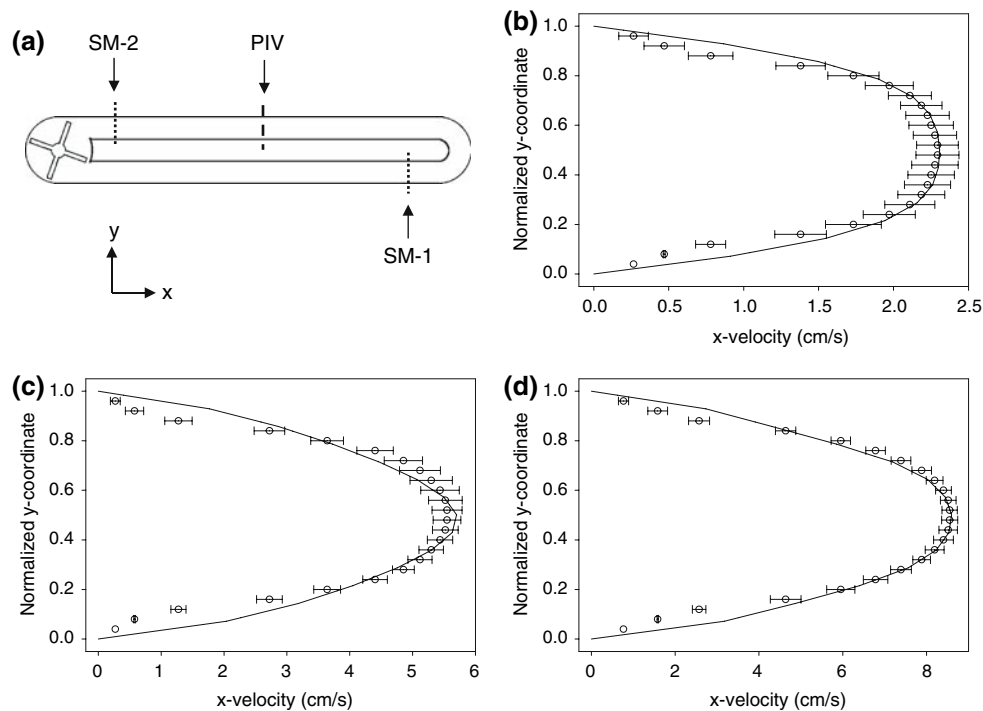
FIGURE 5. Two-dimensional CFD model and PIV experimental validation results. (a) Schematic of the 2D model, which consisted of ~50,000 dynamic fluid elements. The median vertical cross-section at which 2D CFD simulations were compared with PIV measurements is indicated (PIV), The location of the surface monitors (SM-1, SM-2) used to demonstrate convergence are also indicated. These locations also define the extension of the 3D model used. (b) CFD predictions (solid lines) and PIV experimental measurements (open circles) of the *x*-component velocity profile for 1000; (c) 1500; and (d) 2000 rpm paddlewheel rotational velocities. Similar agreement was found for velocity profiles at 350 and 500 rpm (data not shown). Depicted velocity profiles were taken at a dynamic viscosity (μ) of 0.0076 dyne-s/cm^2 corresponding with the viscosity of water (and approximately that of culture medium) at 37 °C, and were averaged over 10 PIV realizations. *Y*-component velocities were approximately three orders of magnitude less than *x*-component velocities and thus were not considered in the analysis.

was associated with a step increase in the rotational velocity of the paddlewheel from 0 rpm to the constant final rotational velocity. The solver was segregated with implicit formulation, SIMPLE pressure–velocity coupling, and a κ–ε turbulent model was assumed to accommodate the possibility of localized turbulence in the immediate vicinity of the paddlewheel. The density of the fluid was proportionally calculated for a 10% serum (1.025 g/cm^3) solution in culture media (1.008 g/cm^3) and determined to be 1.010 g/cm^3. In virtual experiments involving more viscous fluids the corresponding densities were calculated by assuming that addition of the polysaccharide Dextran 40 to the culture medium at concentrations of 5.5% (w/v) and 9% (w/v) would yield viscosities of ~0.0223 and ~0.037 dyne-s/cm^2, and fluid densities of ~1.016 and ~1.040 g/cm^3, respectively.[1] Convergence was taken as residual values $\leq 10^{-5}$ and confirmed with stability of two surface monitors, the first being the maximum velocity in a cross-section segment downstream to the paddlewheel outflow tract, and the second being the average pressure in a cross-section segment upstream to the paddlewheel inflow channel (Fig. 5a). Upon

achievement of steady state (equal velocity profile throughout three consecutive time steps in a local section) the simulations were interrupted and the velocity profile exported in a determined location of the model. Once the velocity field for each velocity (350, 500, 1000, 1500, 2000 rpm) and viscosity (0.0076, 0.0223, 0.037 dyne-s/cm^2) were solved, velocity profiles located consistently with the first surface monitor were exported from the 2D simulations. 3D velocity profiles were numerically generated by extrusion into the third dimension and directly applied upstream of the tissue specimens in 3D simulations to predict the wall shear stresses on the various specimens (Fig. 6). The 3D model consisted of a partial portion of the real model that excluded the paddlewheel and its casing (i.e., 3D geometry comprised between the two surface monitor locations used in the 2D simulations). The 3D geometry was meshed with ~2 million (2 M) tetrahedral elements (4 nodes each) with size functions applied on each specimen in order to increase the velocity gradient (i.e., shear stress) spatial resolution. As an inlet condition for each simulation we used the local spatial velocity profile (velocity inlet) obtained and adapted
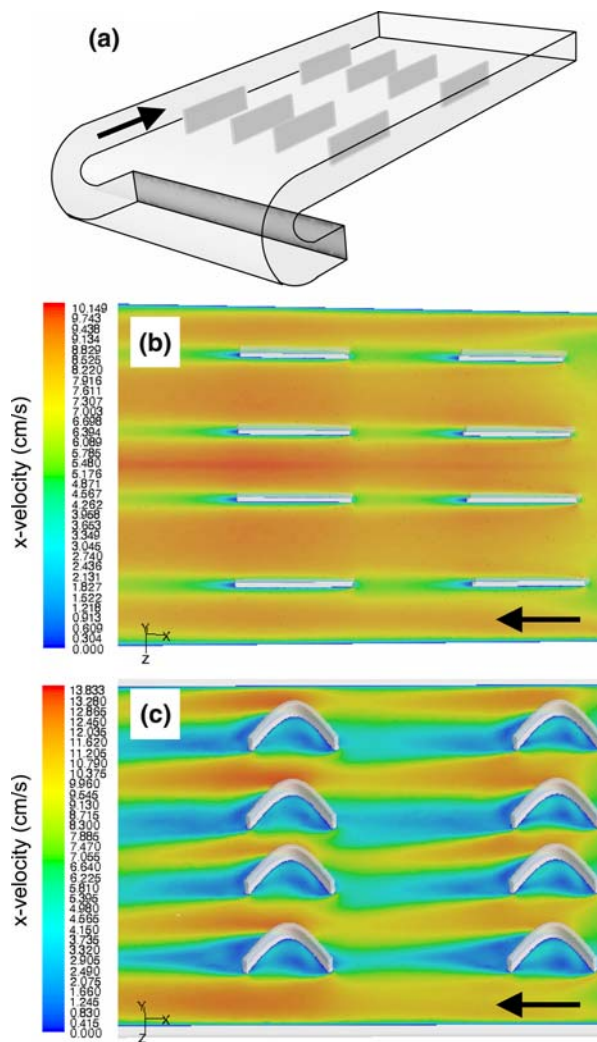
FIGURE 6. Specimen configurations within the three-dimensional CFD model. In the current study a configuration of 8 specimens ($25 \times 7.5 \times 1$ mm) was investigated to simulate a typical specimen load per chamber. (a) Specimens were located in two rows of 4 with the velocity profile extruded from the 2D simulation as an upstream boundary condition (direction of flow indicated by black arrow). (b) Representative steady state velocity profiles at a paddlewheel rotational velocity of 2000 rpm for undeformed and (c) flexed specimens. Note that the color scale bar for (b) ranges from 0 to 10.149 cm/s and for (c) ranges from 0 to 13.833 cm/s.

fields appear to be mesh independent. Thus, a mesh independence study was conducted to verify the suitability of a mesh of 2 M elements. This study was conducted using a paddlewheel rotational velocity of 2000 rpm with specimens in the flexed configuration. The initial mesh size of 2 M elements was both halved (i.e., 1 M elements) and doubled (i.e., 4 M elements), and predicted wall shear stress profiles (averaged across 8 specimens) were compared by correlation coefficient.

RESULTS

FSF Bioreactor Operation

Operation of the bioreactor was straightforward and similar to our previously described cyclic flexure bioreactor.[5,6] Compared with the ~72 mL per chamber capacity of our previous cyclic flexure bioreactor, the ~300 mL per chamber operating capacity of the FSF bioreactor will allow for a longer time between culture medium changes. Loading scaffold specimens into the FSF was simplified by the spiral-bound gripping method (Fig. 3a). Using sterile forceps, the stainless steel spiral grips could be positioned on the posts within the FSF with relative ease beneath a laminar flow hood. Based on the standard specimen geometry of $25 \times 7.5 \times 1$ mm, a full specimen load (i.e., 12 specimens per chamber), and the constraints imposed by the FSF bioreactor chamber dimensions and specimen spacing, specimens could be subjected to a maximum $\Delta\kappa$ of ~50 mm^{-1} and maximum tensile strain of ~75%. Higher tensile strains (up to ~400%) are theoretically possible under a reduced loading configuration of 6 specimens per chamber. A study was undertaken to measure the inter-specimen variability in $\Delta\kappa$ by analysis of images of scaffolds in the flexed configuration. For a programmed $\Delta\kappa$ value of 0.277 mm^{-1}, the experimentally measured value was 0.2747 ± 0.012 mm^{-1} (range 0.221–0.315 mm^{-1}), and for a programmed $\Delta\kappa$ value of 0.554 mm^{-1}, the experimentally measured value was 0.5598 ± 0.024 mm^{-1} (range 0.440–0.63 mm^{-1}).

2D CFD Simulations and Particle Image Velocimetry

The 2D simulations were run at 5 different paddlewheel rotational velocities for the standard culture medium dynamic viscosity ($\mu = 0.0076$ dyne-s/cm^2) (Fig. 5), and at the lowest and highest velocities for two higher viscosities ($\mu = 0.0223$ and $\mu = 0.037$ dyne-s/cm^2) (data not shown). For the standard culture medium viscosity, PIV measurements averaged over 10 realizations corresponded well with CFD predictions (Figs. 5b–d). The highest viscosity value corresponds with the viscosity of blood at a physiologic shear rate,

from the respective 2D simulation. The outlet section had an outflow condition. The simulations for each of the mentioned rpm and viscosities were performed in steady state. The solver was segregated with implicit formulation, SIMPLE pressure–velocity coupling and a laminar flow model. Convergence criteria included residual values $\leq 10^{-5}$ and stability of the surface monitors represented by the average shear stress in each specimen. Prakash and Ethier[20] previously established that considerable care must be taken in confirming the mesh independence of wall shear stress data, as significant errors can arise even when velocity

and can potentially be simulated by adding the appropriate concentration of Dextran 40.[14] Results indicated that viscous energy losses along the length of the fluid flow circuit resulted in significantly decreased fluid velocities with increased fluid viscosity.

3D CFD Simulations

The mesh independence study indicated that a mesh of 2 M elements (Fig. 7a) was sufficient to capture the essential behavior of the model. A comparison of the average wall shear stress profiles extracted from the mid-height plane (Fig. 7b) of the flexed specimens yielded a correlation coefficient of 0.9354 between the 1 and 2 M element mesh results, and a correlation coefficient of 0.9971 between the 2 and 4 M element meshes (Fig. 7c). All subsequent data were generated utilizing the 2 M element mesh. The Reynolds number (averaged over the 3D model flow circuit) and average shear stress per specimen was plotted as a function of paddlewheel rotational velocity (Fig. 8). At the standard culture medium viscosity and a paddlewheel rotational velocity of 2000 rpm, the average predicted wall shear stress was 1.145 ± 0.038 dyne/cm^2 for specimens in the undeformed configuration and ~59% higher (1.821 dyne/cm^2) for specimens in the quasi-static flexed configuration. Inter-specimen variations in the predicted shear stress were not significant for either the undeformed or flexed configurations (Table 1 and Fig. 9). Intra-specimen variations in the predicted shear stress were observed in both the undeformed (Fig. 9a) and flexed (Figs. 9b,c) configurations. In the undeformed specimens, elevated shear stresses were primarily localized to the upstream edge. In the flexed specimens, shear stresses were elevated on the convex side of the specimen relative to the concave side. Predicted velocity vector fields demonstrated the formation of recirculation zones within the concavity demarcated by the flexed specimens and downstream of the specimens on the convex side (Fig. 10).

DISCUSSION

Semilunar heart valves are subjected to three major modes of mechanical loading due to pulsatile blood flow: tensile loading during valve closure, flexural loading during the opening and closing phases, and fluid shear stress during ventricular ejection. In the native valve *in vivo*, and in a TEHV cultivated in a pulsatile flow bioreactor *in vitro*, the three major modes of mechanical loading are inextricably coupled (e.g., pressure-flow relationship), thus precluding isolation of the independent effects of any individual
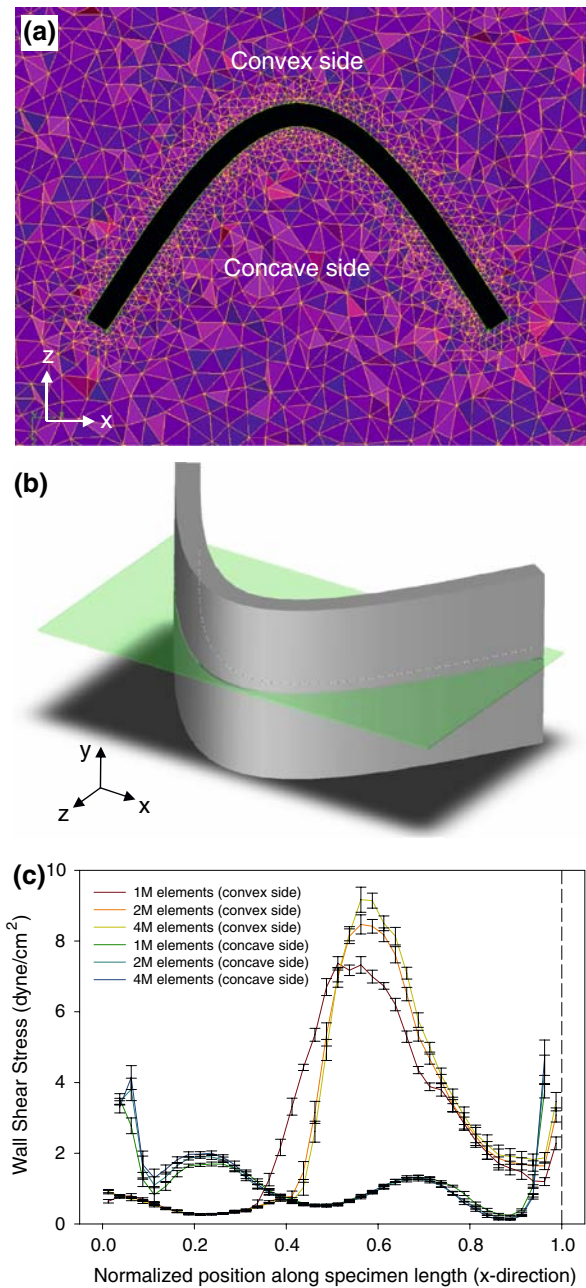

FIGURE 7. Mesh independence study. For the mesh independence study, 3D simulations were run at a paddlewheel rotational velocity of 2000 rpm and with specimens in the flexed configuration to maximize variations in wall shear stress. (a) Image of the 2 million (M) element mesh chosen for generating data (1 and 4 M element meshes not shown). The convex and concave sides of the flexed specimen are indicated. (b) Schematic illustrating the mid-height plane (green plane) from which wall shear stress profiles were extracted for comparison. (c) Comparison of average wall shear stress profiles generated utilizing 1, 2, and 4 M element meshes. For each profile, wall shear stresses were averaged across the eight specimens. Upstream edge is indicated (dashed line). Error bars indicate standard error.

mechanical factor. In the FSF bioreactor these candidate modes of mechanical stimulation can be decoupled to a much greater degree, allowing for relatively
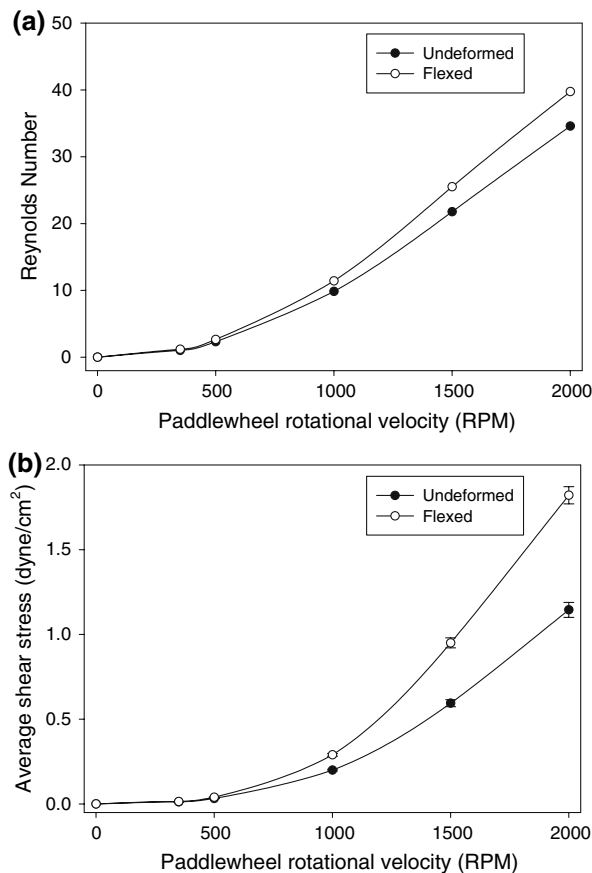
FIGURE 8. Three-dimensional CFD model results. (a) The CFD predicted Reynolds number vs. paddlewheel rotational velocity. Note that Reynolds number values were well within the laminar flow region (<1000) within the vicinity of the specimens. (b) The CFD predicted average fluid shear stress per specimen vs. paddlewheel rotational velocity. The dynamic viscosity simulated ($\mu = 0.0076$ dyne-s/cm^2) corresponded to water (and culture medium) at 37 °C.

independent control of tensile, flexural, or fluid shear stress loading.

Specimen Mounting

In the current study a novel "spiral-bound" specimen mounting technique was developed in which tissue or scaffold specimens are threaded with small diameter wire spirals through which pins are inserted to couple the tissue to either the floor of the bioreactor chamber or to the linear actuator. The spiral-bound method is well-suited for scaffold preparation, as wire spirals can be threaded onto scaffolds prior to scaffold sterilization, thus minimizing engineered tissue handling following cell seeding. The utility of this method was demonstrated in a concurrent study utilizing the FSF bioreactor in which engineered heart valve tissues prepared by seeding 50:50 blend nonwoven

PGA/PLLA scaffolds with ovine BMSC were successfully gripped for periods of 1 and 3 weeks.[8]

Paddlewheel Flow Generation

The FSF bioreactor incorporated a novel magnetically coupled paddlewheel to generate flow. In contrast to previous laminar flow[13] and pulsatile flow[12] bioreactors designed for stimulating engineered tissues, the FSF bioreactor thus allows fluid flow and specimen deformation to be controlled independently. This novel feature is important for differentiating between the effects of flow and strain-mediated stimuli. The speed range of the magnetic stirrer (Corning 75 mm immersible stirrer) used in the current version of the FSF bioreactor is 350–2000 rpm. Thus, using experimentally validated CFD models with a culture medium dynamic viscosity equal to that of water (0.0076 dyne-s/cm^2 at 37 °C), the average shear stress range generated in the FSF bioreactor for undeformed specimens was predicted to be ~0.0125–1.1505 dyne/cm^2 and for specimens under a quasi-static state of flexural deformation was ~0.0143–1.821 dyne/cm^2. While this range of shear stresses is much lower than the physiological shear stresses to which a native aortic valve is exposed to during systole (3–79 dyne/cm^2; Weston *et al.*[24]), studies have demonstrated that shear stresses in this relatively low range can affect collagen concentration in engineered cardiovascular tissues (e.g., ~50% increase in hydroxyproline concentration upon 7 days exposure to ~0.066 dyne/cm^2, followed by a step change to ~0.13 dyne/cm^2 for an additional 7 days; Jockenhoevel *et al.*[13]). (Note that we estimated the shear stresses generated in the study by Jockenhoevel *et al.* from the dimensions of their laminar flow chamber using the equation $\tau_w = (6\,\mu Q)/(bh^2)$,[15] in which Q is the flow rate, b is the width of the rectangular flow chamber, and h is the height of the rectangular flow chamber).

CFD Study Limitations

The CFD studies undertaken herein were intended to provide a reasonable estimate of the average shear stresses experienced by engineered heart valve tissue specimens within the FSF bioreactor. One potential limitation of these CFD studies was the assumption of a closed flow circuit. In the actual FSF bioreactor there is a fluid–air interface over a significant portion of the flow circuit to allow for specimen loading and oxygenation. In pilot CFD studies we attempted to approximate the influence of this fluid–air interface by setting a "zero shear" boundary condition on this interfacial area. A comparison of average wall shear stresses and shear stress profiles between the closed

TABLE 1. Inter-specimen variation in fluid shear stress as a function of specimen position within the FSF bioreactor chamber, specimen shape (i.e., undeformed or flexed), and paddlewheel rotational velocity.

Position	Shape	350 rpm τ (dyne/cm^2)	500 rpm τ (dyne/cm^2)	1000 rpm τ (dyne/cm^2)	1500 rpm τ (dyne/cm^2)	2000 rpm τ (dyne/cm^2)
Inflow wall	Undeformed	0.012 ± 0.006 (3×10^{-4}–0.059)	0.032 ± 0.018 (7×10^{-4}–0.168)	0.202 ± 0.129 (0.004–1.122)	0.602 ± 0.401 (0.011–3.306)	1.157 ± 0.765 (0.027–6.147)
	Flexed	0.013 ± 0.017 (3×10^{-5}–0.072)	0.037 ± 0.046 (5×10^{-5}–0.211)	0.283 ± 0.340 (0.003–1.634)	0.889 ± 1.034 (0.003–4.541)	1.698 ± 1.919 (0.005–8.623)
Inflow center	Undeformed	0.013 ± 0.006 (4×10^{-4}–0.055)	0.034 ± 0.018 (8×10^{-4}–0.156)	0.221 ± 0.142 (0.003–1.070)	0.676 ± 0.441 (0.011–3.181)	1.311 ± 0.839 (0.024–5.717)
	Flexed	0.014 ± 0.018 (3×10^{-5}–0.083)	0.040 ± 0.050 (7×10^{-4}–0.232)	0.297 ± 0.351 (0.006–1.631)	0.962 ± 1.283 (0.003–4.564)	1.845 ± 2.129 (0.013–9.938)
Outflow wall	Undeformed	0.012 ± 0.006 (4×10^{-4}–0.061)	0.031 ± 0.016 (9×10^{-4}–0.187)	0.186 ± 0.102 (0.004–1.569)	0.541 ± 0.296 (0.013–4.966)	1.020 ± 0.552 (0.030–9.340)
	Flexed	0.015 ± 0.018 (5×10^{-5}–0.081)	0.042 ± 0.052 (1×10^{-4}–0.266)	0.304 ± 0.359 (0.004–1.880)	0.977 ± 1.317 (0.004–5.298)	1.868 ± 2.133 (0.011–9.867)
Outflow center	Undeformed	0.013 ± 0.006 (4×10^{-4}–0.058)	0.032 ± 0.016 (7×10^{-4}–0.179)	0.194 ± 0.103 (0.003–1.516)	0.579 ± 0.311 (0.011–4.666)	1.114 ± 0.590 (0.026–8.606)
	Flexed	0.015 ± 0.018 (6×10^{-5}–0.095)	0.041 ± 0.051 (1×10^{-4}–0.238)	0.274 ± 0.333 (0.002–1.551)	0.975 ± 1.311 (0.004–5.112)	1.875 ± 2.154 (0.015–8.656)

Average wall shear stress (τ) values are reported in units of dyne/cm^2 with corresponding standard deviations (σ). For each specimen the range of observed τ values is given in parentheses. Specimens were located symmetrically about the central axis of each FSF bioreactor chamber, and thus only 4 of the 8 specimens are presented above.

model and the "zero shear" model suggested that the effects of the fluid–air interface were negligible (data not shown). An improved estimate of the fluid dynamic behavior of the FSF bioreactor could potentially be derived by explicitly simulating the fluid–air interface, however such simulations were beyond the scope of the current study.

FSF Bioreactor Cultivation of Engineered Heart Valve Tissues

In a concurrent study[8] we utilized the FSF bioreactor to investigate the independent and coupled effects of cyclic flexure and laminar flow on engineered heart valve tissue formation. Ovine BMSC were isolated from juvenile sheep as described previously[19,23] and expanded in a basal culture medium consisting of Dulbecco's Modified Eagle's Medium with 4.5 g/L glucose and L-glutamine (GIBCO[TM], Invitrogen Corporation, Grand Island, NY) supplemented with 10% fetal bovine serum (GIBCO[TM]) and 1% antibiotic-antimycotic (GIBCO[TM]). Nonwoven 50:50 blend poly(glycolic acid) and poly(L-lactic acid) scaffolds (~25 × 7.5 × 1 mm; Albany International Research, Mansfield, MA) were prepared beforehand by threading each side with stainless steel wire spirals as described above and sterilized by ethylene oxide. After sufficient numbers were obtained, BMSC were dynamically seeded onto scaffolds at a density of ~17 × 10^6 cells/cm^2 for 30 h. BMSC-seeded scaffolds were maintained in static culture for 4 days prior to loading in the FSF bioreactor. BMSC-seeded scaffolds were incubated under static ($n = 12$), cyclic flexure (1 Hz, $\Delta\kappa = 0.554$ mm^{-1}; $n = 12$), laminar flow ($\tau = 1.1505$ dyne/cm^2; $n = 12$) and combined flex-flow ($n = 12$) conditions for 1 ($n = 6$) and 3 ($n = 6$) weeks and then characterized by effective stiffness (E) testing, DNA and extracellular matrix assays, histology, immunohistochemistry, and scanning electron microscopy (SEM). By 3 weeks, the flex-flow group exhibited dramatically accelerated tissue formation compared with other groups, including a DNA concentration of 47.0 ± 4.8 μg/g wet weight, a modest decrease in S-GAG concentration from 1-week values to 1919 ± 54 (-23%; $p < 0.05$) μg/g wet weight, a collagen concentration of 844 ± 278 μg/g wet weight, and an E value of 948 ± 233 kPa. Of particular note, the collagen and E values were not significantly different from vascular smooth muscle cell (SMC) seeded scaffolds incubated under independent cyclic flexure conditions (893 ± 133 μg/g wet weight and 978 ± 228 kPa, respectively),[6] suggesting that mechanical conditioning regimens for BMSC-seeded TEHV can be optimized to yield results comparable to SMC-seeded TEHV. SEM provided additional evidence for accelerated tissue formation in the flex-flow group that was corroborated by histology. These previous results demonstrated the suitability of the FSF bioreactor for cultivating viable engineered heart valve tissues. Moreover, we demonstrated that cyclic flexure and laminar flow can synergistically accelerate BMSC-mediated tissue formation, providing a basis for the rational design of bioreactor conditioning regimens for BMSC-seeded TEHV.
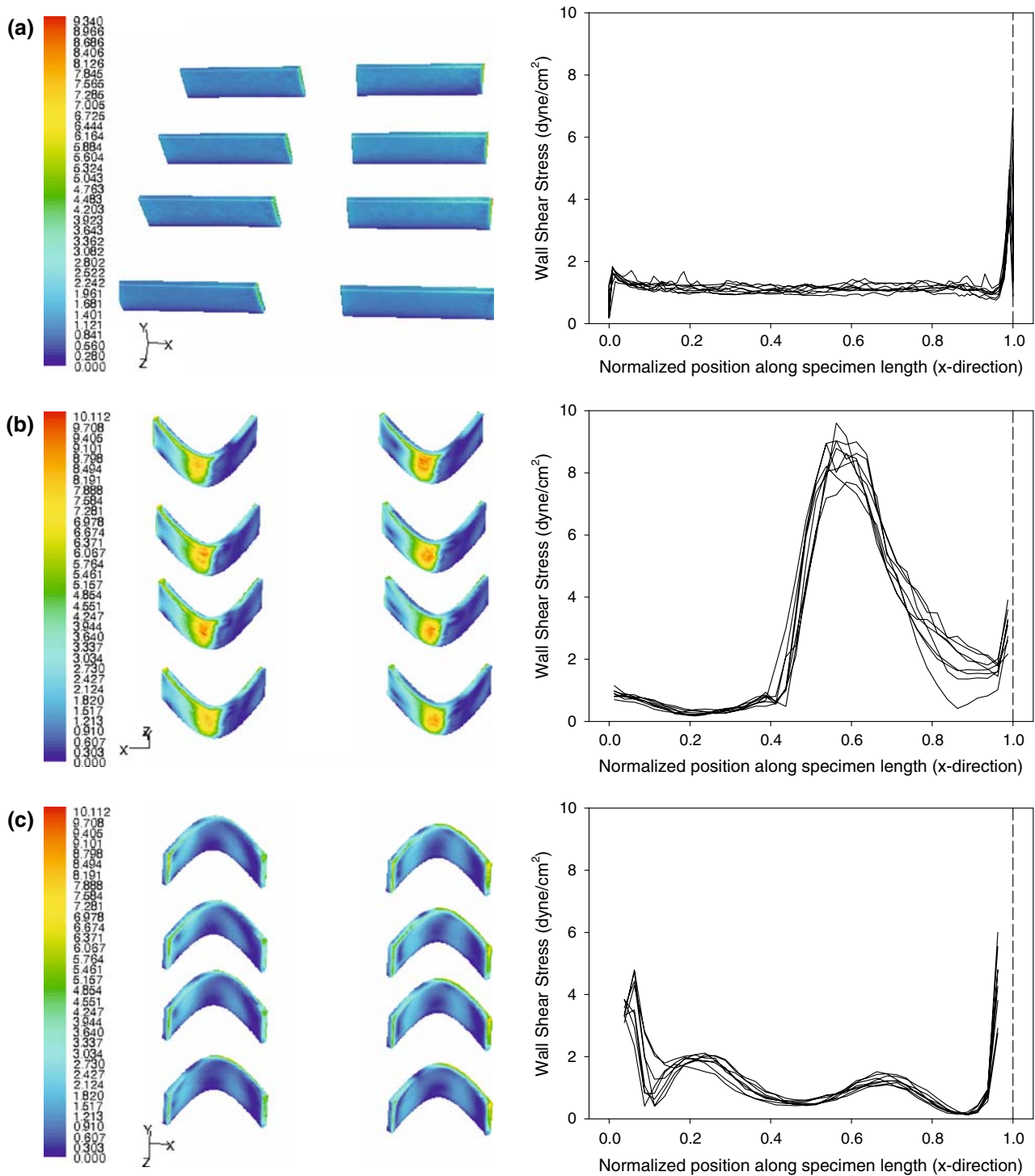
FIGURE 9. Inter- and intra-specimen variability in wall shear stress at a paddlewheel rotational velocity of 2000 rpm. (a) Specimens in the undeformed configuration exhibited low inter-specimen variability in wall shear stress (see also Table 1), with intra-specimen variability along the specimen length primarily limited to elevated values at the upstream edge (dashed line) and decreased values at the downstream edge. Note that in the right-hand panel wall shear stress profiles from both sides of the specimen are plotted together. (b) For flexed specimens, wall shear stresses on the convex side were elevated at the upstream edge (dashed line) and maximal immediately upstream of the point of maximum specimen curvature. Inter-specimen variability was slightly higher than in undeformed specimens (see also Table 1). (c) On the concave side, wall shear stresses were maximal at the upstream (dashed line) and downstream edges and minimal near the point of maximum specimen curvature. Collectively, inter- and intra-specimen variability were lower at lower paddlewheel rotational velocities (data not shown; see Table 1) Note that the color scale bar for (a) ranges from 0 to 9.34 dyne/cm², and for (b) and (c) ranges from 0 to 10.112 dyne/cm².
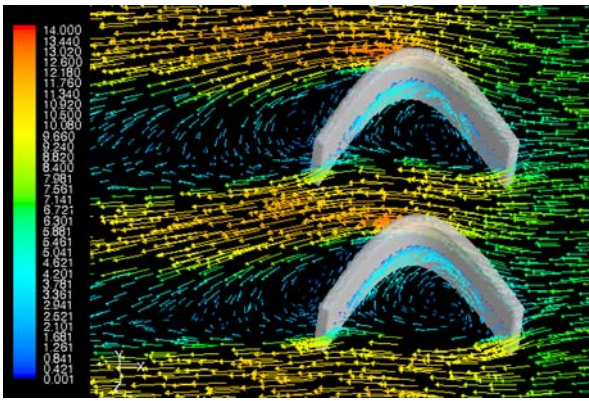
FIGURE 10. Fluid recirculation around flexed specimens. Velocity vector fields at a paddlewheel rotational velocity of 2000 rpm demonstrated the existence of recirculation zones within the concavity demarcated by the flexed specimens, as well as downstream of the flexed specimens on the convex side. Note that the color bar scale ranges from 0 to 14 cm/s.

Limitations of the Current FSF Bioreactor Design and Potential Future Modifications

The FSF bioreactor in its current form, while providing a satisfactory solution to the testing of multiple engineered heart valve tissue specimens, continues to have certain limitations which we aim to address in future design modifications. In particular, we initially hypothesized that the shear stresses could be increased by increasing the viscosity of the culture medium to approximate the viscosity of blood at physiological shear rates (~0.037 dyne-s/cm^2 at 37 °C) maintaining the same level of rotational speed for the paddlewheel. This could potentially have been accomplished by adding the appropriate amount of the polysaccharide Dextran-40 to the culture medium. For example, a 10% solution of Dextran 40 with a viscosity of ~0.063 dyne-s/cm^2 at 23 °C was previously utilized to study the effects of shear stress on red blood cells.[14] We found, however, that the sole increase in viscosity introduced energetic losses in the fluid stream leading to significant decreases in velocities due to the intrinsic centrifugal characteristics of the pump used (spinning paddlewheel). The reduction in velocity peaks (i.e., reduction in velocity gradients at the specimen level) exceeded the increase in shear stresses due to an increase in dynamic viscosity; this abrogated any increase of fluid shear stress at the specimens. Thus, a simpler way of increasing the fluid shear stress range of the FSF would be to incorporate a faster motor for spinning the paddlewheel. Preliminary CFD simulations were conducted to predict the shear stresses achievable using a stirrer motor operating at either 5000 or 10,000 rpm. Tentatively these simulations suggest that average specimen wall shear stress values of 8.79 and 25.63 dyne/cm^2, respectively, could be achieved for flexed specimens, however the incorporation of a faster motor could require modifications of the paddlewheel and/or flow circuit design to maintain laminar flow and avoid cavitation.

It was recognized that inter-specimen variability in shear stress could be reduced by only loading one row of specimens (i.e., either the upstream or the downstream row), and by increasing the width of the chamber to both accommodate more specimens per row and to reduce proximity effects associated with the chamber wall. Another potential limitation involves the mechanism utilized for subjecting specimens to cyclic flexural deformations. In the FSF bioreactor, specimens are essentially buckled to provide flexural deformation. In our recent study on the effects of cyclic flexure and laminar flow on BMSC-mediated engineered tissue formation,[8] BMSC-seeded nonwoven 50:50 PGA/PLLA scaffolds (~1 mm thick) exhibited sufficient flexural rigidity to retain their flexed shape when simultaneously subjected to continuous laminar flow. Thinner specimens (e.g., native heart valve leaflet tissue) exhibiting much lower flexural rigidities could potentially undergo complex deformations in response to combined flexure and flow.

Conclusion

In conclusion, in the current study a novel bioreactor was developed in which flexure, stretch, and flow (FSF) stimuli can be independently controlled. Specimens are gripped within the FSF bioreactor via a novel "spiral-bound" tissue-gripping technique, and flow is generated via a magnetically coupled paddlewheel. The shear stress ranges of ~0.0125–1.1505 dyne/cm^2 for undeformed specimens and ~0.0143–1.821 dyne/cm^2 for flexed specimens, while lower than the physiological regime, are well within the range of shear stresses previously shown to stimulate tissue formation in TEHV. The FSF bioreactor is uniquely suited for developing optimized mechanical conditioning regimes for TEHV due to the ability to assess a large number of specimens (up to 24 simultaneously) under well-controlled mechanical stimuli combinations.

REFERENCES

[1] Akashi, N., J. I. Kushibiki, and F. Dunn. Measurements of acoustic properties of aqueous dextran solutions in the VHF/UHF range. *Ultrasonics* 38(9):915–919, 2000.

[2] Budilarto, S. G., B. J. Frankowski, B. G. Hattler, and W. J. Federspiel. Flow visualization study of a pulsating respiratory assist catheter. *Asaio J.* 51(6):673–680, 2005.

[3] Costa, K. D., E. J. Lee, and J. W. Holmes. Creating alignment and anisotropy in engineered heart tissue: role of boundary conditions in a model three-dimensional culture system. *Tissue Eng.* 9(4):567–577, 2003.

[4] Driessen, N. J., C. V. Bouten, and F. P. Baaijens. Improved prediction of the collagen fiber architecture in the aortic heart valve. *J. Biomech. Eng.* 127(2):329–336, 2005.

[5] Engelmayr, G. C., Jr., D. K. Hildebrand, F. W. Sutherland, J. E. Mayer, Jr., and M. S. Sacks. A novel bioreactor for the dynamic flexural stimulation of tissue engineered heart valve biomaterials. *Biomaterials* 24(14):2523–2532, 2003.

[6] Engelmayr, G. C., Jr., E. Rabkin, F. W. Sutherland, F.J. Schoen, J. E. Mayer, Jr., and M. S. Sacks. The independent role of cyclic flexure in the early *in vitro* development of an engineered heart valve tissue. *Biomaterials* 26(2):175–187, 2005.

[7] Engelmayr, G. C., Jr., and M. S. Sacks. A structural model for the flexural mechanics of nonwoven tissue engineering scaffolds. *J. Biomech. Eng.* 128(4):610–622, 2006.

[8] Engelmayr, G. C., Jr., V. L. Sales, J. E. Mayer, Jr., and M. S. Sacks. Cyclic flexure and laminar flow synergistically accelerate mesenchymal stem cell-mediated engineered tissue formation: Implications for engineered heart valve tissues. *Biomaterials* 27(36):6083–6095, 2006.

[9] Fu, P., R. Sodian, C. Luders, T. Lemke, L. Kraemer, M. Hubler, Y. Weng, S. P. Hoerstrup, R. Meyer, and R. Hetzer. Effects of basic fibroblast growth factor and transforming growth factor-beta on maturation of human pediatric aortic cell culture for tissue engineering of cardiovascular structures. *Asaio J.* 50(1):9–14, 2004.

[10] Hildebrand, D. K., Z. J. Wu, J. E. Mayer, Jr., and M. S. Sacks. Design and hydrodynamic evaluation of a novel pulsatile bioreactor for biologically active heart valves. *Ann. Biomed. Eng.* 32(8):1039–1049, 2004.

[11] Hoerstrup, S. P., R. Sodian, S. Daebritz, J. Wang, E. A. Bacha, D. P. Martin, A. M. Moran, K. J. Guleserian, J. S. Sperling, S. Kaushal, J. P. Vacanti, F. J. Schoen, and J. E. Mayer, Jr. Functional living trileaflet heart valves grown *in vitro*. *Circulation* 102(19 Suppl. 3):III44–III49, 2000.

[12] Hoerstrup, S. P., R. Sodian, J. S. Sperling, J. P. Vacanti, and J. E. Mayer, Jr. New pulsatile bioreactor for *in vitro* formation of tissue engineered heart valves. *Tissue Eng.* 6(1):75–79, 2000.

[13] Jockenhoevel, S., G. Zund, S. P. Hoerstrup, A. Schnell, and M. Turina. Cardiovascular tissue engineering: a new laminar flow chamber for *in vitro* improvement of mechanical tissue properties. *Asaio J.* 48(1):8–11, 2002.

[14] Kameneva, M. V., G. W. Burgreen, K. Kono, B. Repko, J. F. Antaki, and M. Umezu. Effects of turbulent stresses upon mechanical hemolysis: experimental and computational analysis. *Asaio J.* 50(5):418–423, 2004.

[15] Lee, A. A., D. A. Graham, S. Dela Cruz, A. Ratcliffe, and W. J. Karlon. Fluid shear stress-induced alignment of cultured vascular smooth muscle cells. *J. Biomech. Eng.* 124(1):37–43, 2002.

[16] Mol, A., C. V. Bouten, G. Zund, C. I. Gunter, J. F. Visjager, M. I. Turina, F. P. Baaijens, and S. P. Hoerstrup. The relevance of large strains in functional tissue engineering of heart valves. *Thorac. Cardiovasc. Surg.* 51(2):78–83, 2003.

[17] Mol, A., N. J. Driessen, M. C. Rutten, S. P. Hoerstrup, C. V. Bouten, and F. P. Baaijens. Tissue engineering of human heart valve leaflets: a novel bioreactor for a strain-based conditioning approach. *Ann. Biomed. Eng.* 33(12):1778–1788, 2005.

[18] Nugent, H. M., and E. R. Edelman. Tissue engineering therapy for cardiovascular disease. *Circ. Res.* 92(10):1068–1078, 2003.

[19] Pittenger, M. F., A. M. Mackay, S. C. Beck, R. K. Jaiswal, R. Douglas, J. D. Mosca, M. A. Moorman, D. W. Simonetti, S. Craig, and D. R. Marshak. Multilineage potential of adult human mesenchymal stem cells. *Science* 284(5411):143–147, 1999.

[20] Prakash, S., and C. R. Ethier. Requirements for mesh resolution in 3D computational hemodynamics. *J. Biomech. Eng.* 123(2):134–144, 2001.

[21] Rabkin, E., S. P. Hoerstrup, M. Aikawa, J. E. Mayer, Jr., and F. J. Schoen. Evolution of cell phenotype and extracellular matrix in tissue-engineered heart valves during *in vitro* maturation and *in vivo* remodeling. *J. Heart Valve Dis.* 11(3):308–314, 2002: discussion 314.

[22] Sacks, M. S. Biomechanics of native and engineered heart valve tissues. In: Functional Tissue Engineering, edited by F. Guilak, D. L. Butler, S. Goldstein, and D. Mooney. New York: Spring-Verlag, 2003.

[23] Sutherland, F. W., T. E. Perry, Y. Yu, M. C. Sherwood, E. Rabkin, Y. Masuda, G. A. Garcia, D. L. McLellan, G. C. Engelmayr, Jr., M. S. Sacks, F. J. Schoen, and J. E. Mayer, Jr.. From stem cells to viable autologous semilunar heart valve. *Circulation* 111(21):2783–2791, 2005.

[24] Weston, M. W., D. V. LaBorde, and A. P. Yoganathan. Estimation of the shear stress on the surface of an aortic valve leaflet. *Ann. Biomed. Eng.* 27(4):572–579, 1999.